Applied Energy 352 (2023) 121988

Contents lists available at ScienceDirect

Applied Energy

journal homepage: www.elsevier.com/locate/apenergy

Potential of agrivoltaics systems into olive groves in the Mediterranean region

Álvaro Fernández-Solas [a,*], Ana M. Fernández-Ocaña [b], Florencia Almonacid [a], Eduardo F. Fernández [a]

[a] Advances in Photovoltaic Technology (AdPVTech), CEACTEMA, University of Jaén, Las Lagunillas Campus, Jaén 23071, Spain
[b] Departamento de Biología Animal, Biología Vegetal y Ecología, Facultad de Ciencias Experimentales, University of Jaén, Las Lagunillas Campus, Jaén 23071, Spain

HIGHLIGHTS

- The potential integration of photovoltaics into olive groves is assessed.
- Representative locations in top olive producers Mediterranean countries are selected.
- Suitable PV transparency levels between 57% and 71% are found.
- The average generation with the proposed APV configuration is approximately 65 kWh/year per m^2 of ground.
- These agrivoltaics systems could lead to the creation of >560,000 jobs.

ARTICLE INFO

Keywords:
Photovoltaic
Agrivoltaics
Olive farming
Semi-transparent modules
Mediterranean region
Potential evaluation

ABSTRACT

Agrivoltaics systems have emerged as an approach to alleviate competition for land use between food and energy production. Conducting a thorough analysis of the impact that shading from PV modules can have on crops is crucial for the correct design of the system, as excessive shading can lead to important crop yield reductions. This paper focuses on integrating agrivoltaics systems within super-intensive olive groves in the Mediterranean region. A dual model is used to calculate the suitable transparency of PV modules, representing the area not occupied by PV cells. This model customizes the results based on the site's meteorological parameters and the photosynthetic light-response curve of the olive cultivar. The results indicate that transparency levels vary between 0.57 and 0.71, with the lowest values observed in locations with higher solar radiation, such as Egypt and Tunisia. Using these transparency values and typical 20%-efficiency monocrystalline silicon modules, the annual average energy generation per m^2 in the selected locations is 65.9 kWh. Another finding reveals that optimizing the model by considering only the months corresponding to the olive growth cycle can reduce the required transparency, thereby increasing the installed PV capacity by up to 3.5%. Furthermore, the potential deployment of these systems is evaluated in terms of installed PV capacity, energy generation, CO_2 emissions and job creation. The calculations show that installing agrivoltaics systems into 1% of the total olive surface area in the Mediterranean region would: (i) result in a 2.5% increase in the global PV capacity, (ii) generate 1.8% of the current electricity demand in the selected Mediterranean countries, (iii) avoid the emissions of 4 Mt. (CO_2) per year, and (iv) create around 560,000 jobs.

1. Introduction

The urgent need to reduce the energy dependence on fossil fuels to meet the Sustainable Development Goals (SDGs) [1] related to affordable and clean energy generation (SDG No. 7) and climate change action (SDG No. 13) has promoted a massive deployment of solar energy worldwide [2]. The firm commitment towards this kind of renewable energy can be accounted for two main reasons: (i) its low cost compared to other renewable technologies and (ii) energy production can be achieved in a massive scale through large solar farms. This latter fact involves the occupation of wide land surfaces, which, in some cases, has

* Corresponding author.
E-mail addresses: afsolas@ujaen.es (Á. Fernández-Solas), amocana@ujaen.es (A.M. Fernández-Ocaña), facruz@ujaen.es (F. Almonacid), eduardo.fernandez@ujaen.es (E.F. Fernández).

https://doi.org/10.1016/j.apenergy.2023.121988
Received 31 March 2023; Received in revised form 25 July 2023; Accepted 17 September 2023
Available online 29 September 2023
0306-2619/

Nomenclature

Symbols

A	Area of the module, m^2
AOIF	Angle of incidence factor, unitless
c	Speed of light constant, m/s
C&I	Jobs linked to construction and installation of PV systems, unitless
E	Spectral irradiance, $W/(m^2 \cdot nm)$
EF_i	Employment factor, jobs/MWp
F_0	Minimal fluorescence in dark-adapted conditions, a.u.
F_0’	Minimal fluorescence in light-adapted conditions, a.u.
F_m	Maximal fluorescence in dark-adapted conditions, a.u.
F_m’	Maximal fluorescence in light-adapted conditions, a.u.
G	Global irradiance, W/m^2
GCR	Ground coverage ratio, unitless
h	Planck’s constant, eV·s
I_{sat}	Light saturation point, μmol $/(m^2 s)$
k_{CO2}	CO_2 emission coefficient, kg/kWh
k_{PV}	APV penetration constant, unitless
N_A	Avogadro’s constant, mol^{-1}
O&M	Jobs linked to operation and maintenance of PV systems, unitless
P/A	Power per unit area, W/m^2
PAR	Photosynthetically active radiation, μmol $/(m^2 s)$
PPFD	Photosynthetic photon flux density, μmol $/(m^2 s)$
PVCCR	Photovoltaic cell coverage ratio, unitless
PVF	Photovoltaic active factor, unitless
PSN	Net photosynthesis rate, mol CO_2/m^2
REM	Regional employment multiplier, unitless
SF	Spectral factor of PV modules, unitless
TF	Thermal factor, unitless
TRF	Transmittance factor, unitless

Greek letters

η	Efficiency, unitless
λ	Wavelength, nm
τ	Spectral transmittance, unitless

Abbreviations

APV	Agrivoltaics
CO_2	Carbon dioxide
FAO	Food and Agriculture Organization
GHG	Greenhouse gases
m-Si	Monocrystalline Silicon
MENA	Middle East and North Africa
OECD	Organization for Economic Cooperation and Development
POA	Plane of Array
PSSI	Photosystem II, also known as water-plastoquinone oxidoreductase
PV	Photovoltaic
PVGIS	Photovoltaic Geographical Information System
SDGs	Sustainable Development Goals
SPECTRL2	Bird Simple Spectral Model
TMY	Typical Meteorological Year

Subscripts

active	Part of the module with photovoltaic cells
c	country
DH	Direct horizontal irradiance
DiffH	Diffuse horizontal irradiance
glass	Part of the module with transparent glass material
m	Maximum chlorophyll fluorescence
plant	Irradiance on the crops
POA	Irradiance on the plane of photovoltaic array
STC	Standard test conditions

caused social acceptance issues [3–5], being the land-use conflict between agricultural activities and energy generation one of the main concerns. A feasible approach to tackle this issue is the dual use of land for both crop cultivation and energy production. This solution is called Agrivoltaics if the energy generation is achieved through photovoltaic (PV) installations. The potential of this approach was highlighted by Adeh et al. [6], as they indicated that the conversion of <1% of the croplands into agrivoltaics systems can completely offset the global energy demand.

Agrivoltaics systems (APV) consist of the combination of a PV generator and an agricultural field. This kind of systems was referenced for the first time in the literature four decades ago [7], but it was not until the last few years, coinciding with the highest growth of PV capacity, when the interest in this approach started to raise. Fig. 1 shows both the evolution of the cumulative installed global PV capacity and the number of studies addressing APV. In the last two years, >200 research publications on the topic were published in Scopus indexed journals. In addition to the increase of land productivity achieved by APV, researchers are also making efforts to find synergies between agriculture and PV installations. The self-consumption of the generated PV energy for irrigation, lighting or heating of greenhouses [8], a more efficient use of water [9,10], and the control of both soil temperature and the light radiation that reaches the crops [11,12] are among the benefits of APV for crop cultivation. In addition, the micro-climate conditions generated by the crops underneath the PV installation can contribute to a reduction in the PV module temperature [13–15], and, thus, improving the PV performance. The positive impact of these synergies is expected to be more relevant in arid regions where the crop yield may rise due to the water savings [16]. Also, the reduction of the stress produced in the

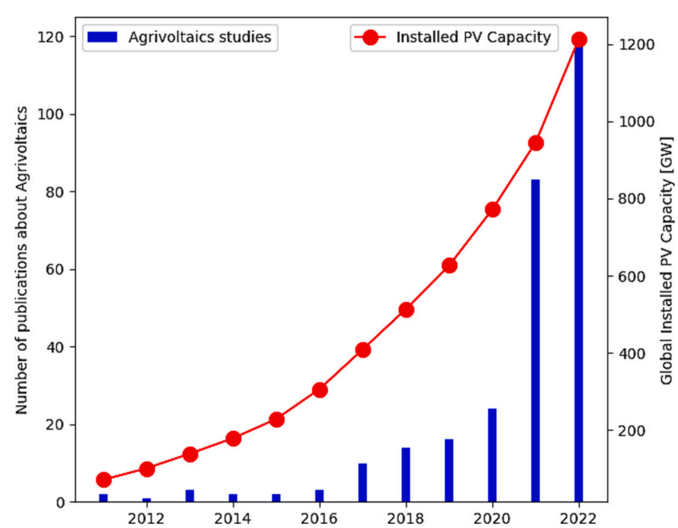

Fig. 1. Evolution of the number of publications related with Agrivoltaics (bar plot: left y-axis) and growth of the global installed PV capacity (line plot: right y-axis) since 2011. The publications data have been obtained by searching in February 2023 for publications on Scopus [17] that contain the following terms in the title, abstract or keywords: “agrivoltaic” OR “agrivoltaics” OR “agri-photovoltaics” OR “agrovoltaics” OR “PV-greenhouse”. Sources of the PV capacity data: [18,19].

plants by an excessive radiation can be attenuated by APV [12].

One of the main important aspects regarding APV is the selection of suitable crops. The principal factor that defines this choice is the tolerance to shade of plants. This is commonly evaluated through photosynthesis-light curves representing the net photosynthesis rate response to photosynthetically active radiation (PAR). From these curves, the saturation irradiance or light saturation point (I_{sat}), which indicates the light intensity at which the net photosynthesis rate reaches its maximum [20], can be obtained. When the incident irradiance exceeds this point, the plant begin to suffer photoinhibition, i.e. their photosynthetic apparatus inhibit the absorption of greater amounts of light to avoid being damaged. This fact frequently occurs in the Mediterranean basin, where in summer, extremely high irradiance and temperature values, which can negatively impact olive groves, are often reached. Therefore, analyzing this information in conjunction with the type of APV system represents a challenge of great interest in modern agriculture. As established by Gorjian et al. [21], APV systems can be classified into two main categories: (i) open APV, and (ii) closed APV. Closed APV essentially refer to PV greenhouses, i.e. greenhouses in which PV modules have been integrated into the roof or walls. Open APV can be divided, according to the PV configuration, in two types: (i) interspace APV, which refer to APV with crop cultivation between the rows of PV modules, and (ii) overhead APV, these are systems in which the crops are grown underneath the PV modules. Cossu et al. [8] evaluated the suitability of different crops for their cultivation in different types of European PV greenhouses. The Japanese "solar sharing" association [22] summarized the most important crops in Japan by considering their light saturation point and their light requirements to provide guidelines for APV design. Another important factor that should be taken into account when assessing the suitability of crops for APV is the sensitivity of these to extreme weather events, such as hail, heavy rainfalls or extreme temperatures. In this way, fruits and berries, which have been demonstrated to be particularly sensitive to tough conditions, can be suitable for APV from an agricultural viewpoint, as a likely yield reduction due to the shading can be counterbalanced with the protection of PV modules that act as shelter [23]. In the case of olive groves, the shade produced by the PV modules could be especially advantageous due to the increase in the frequency of occurrence of droughts and extreme temperatures in areas with a Mediterranean climate in the last decades [24].

Nowadays, and in addition to the evaluation of new approaches on PV greenhouses, which have a non-negligible potential, as evaluated by Fernández et al. [25], the focus should also be put on the integration of PV in already existing land surfaces of orchards or groves. A wide range of studies that addressed the results of open APV systems with different crop types, such as alfalfa [26], broccoli [27], corn [28], wheat [29,30], cucumber [30], lettuce [29,31] or wine grapes [32] are available in the literature. Also, the potential of APV in vineyards has been analyzed: Malu et al. [33] studied the possible energy generation through APV in grape farms in India, which can meet the energy demand of 15 million people, and Padilla et al. [34] evaluated the integration of PV into previously built vineyards structures in a Spanish region.

However, and despite the above mentioned, the integration of PV into arboriculture has not been deeply evaluated, with the particular exception of apples cultivation. There are some experimental APV installations with apple orchards already commissioned [35,36]. In this paper, the potential of APV in already existing olive groves in the Mediterranean area is assessed. The research on this topic can be clearly justified by the large land surface occupied by this perennial, evergreen woody crop with around ten million hectares in the area [37]. So far, there are no operating APV installations in olive groves. Nevertheless, some recent studies suggested the likely feasibility of these systems. Osorio-Aravena et al. [38] identified suitable sites for the implementation of PV plants in the province of Jaén, Spain and discovered that 80% of those sites were placed in olive groves. They mentioned the possibility of evaluating the application of APV with olive trees to increase the PV potential. In [39], APV systems, which would allow farmers to enhance the productivity of their land, were proposed to reduce the social opposition to large PV plants in Jaén. To date, the study presented by Ciocia et al. [40] is the only one that has addressed the modeling of an APV system within an olive grove. The authors proposed a suitable APV configuration for super-intensive olive cultivation, providing rough estimates for both PV energy generation and olive yield. Furthermore, there are indications of increasing interest in the adoption of APV systems within olive groves, as evidenced by planned projects. For instance, a German company expressed intentions to construct three PV plants, totaling 244 MW in capacity, within olive groves located in southern Italy [41]. These proposed systems would feature rows of PV modules interspersed with rows of olive trees, showcasing the growing momentum of APV within the olive farming industry.

This study evaluates the potential integration of PV systems into existing olive groves in the Mediterranean region. The kind of APV system that has been considered is known as "overhead", which, as it was above mentioned, lies in the mounting of PV modules above the crops. This type of APV is suitable for fruit trees. Also, this technology contributes to reducing the soil evaporation [42], which directly translates into a decrease in the water demand. This synergistic effect is expected to cause relevant benefits for olives farmers due to the savings that the lower use of water compared to traditional groves implies, with the consequent saving of energy and the mitigation of stress symptoms in plants due to high temperatures and/or droughts. By following the same methodology described in [25], the most suitable level of transparency of the PV modules for some of the most representative olive cultivars is calculated for the top olive producing Mediterranean countries. In this study, we examine glass PV modules composed of multiple PV cells interspersed within them. Transparency, in this context, refers to the proportionate area of the module that is unoccupied by PV cells. This value is then multiplied by the optical transmittance of the glass to calculate the overall transparency of the module.

Taking the above in mind, some indicators related to aspects, such as the PV capacity, the energy generation, the reduction in greenhouse emissions and the job creation, are calculated to reveal the potential of APV systems in olive groves.

The paper is structured as follows: Section 2 presents the methodology and the criteria that have been considered to conduct the study, Section 3 analyzes the levels of transparency that PV modules should have to minimize the impact of shading on the olive trees, Section 4 shows the potential of overhead APV systems in olive groves in the Mediterranean area; finally, Section 5 recapitulates the main conclusions of the work.

2. Materials and methods

This section describes the methodology used in this work and presents the different inputs of the experimental model that have been employed to calculate the suitable transparency values. Fig. 2 shows a flowchart with the main steps and outputs of the study. The study presents four principal stages: (i) the selection of representative locations, (ii) the experimental characterization of the light response of olive trees, (iii) the application of the dual APV model to obtain the transparency for each location, and (iv) the evaluation of different indicators to highlight the potential of PV systems integration within olive farming. All the stages are explained in detail in the following subsections.

2.1. Identification of representative locations

The choice of the different locations has been made by following a two-stage process. First, a search of the top olive oil producing countries in the most recent 5-year interval with available data (2017–2021) was conducted. This led to the finding that the top-10 is completely occupied by countries located in the Mediterranean region according to the information published by the Food and Agriculture Organization of the

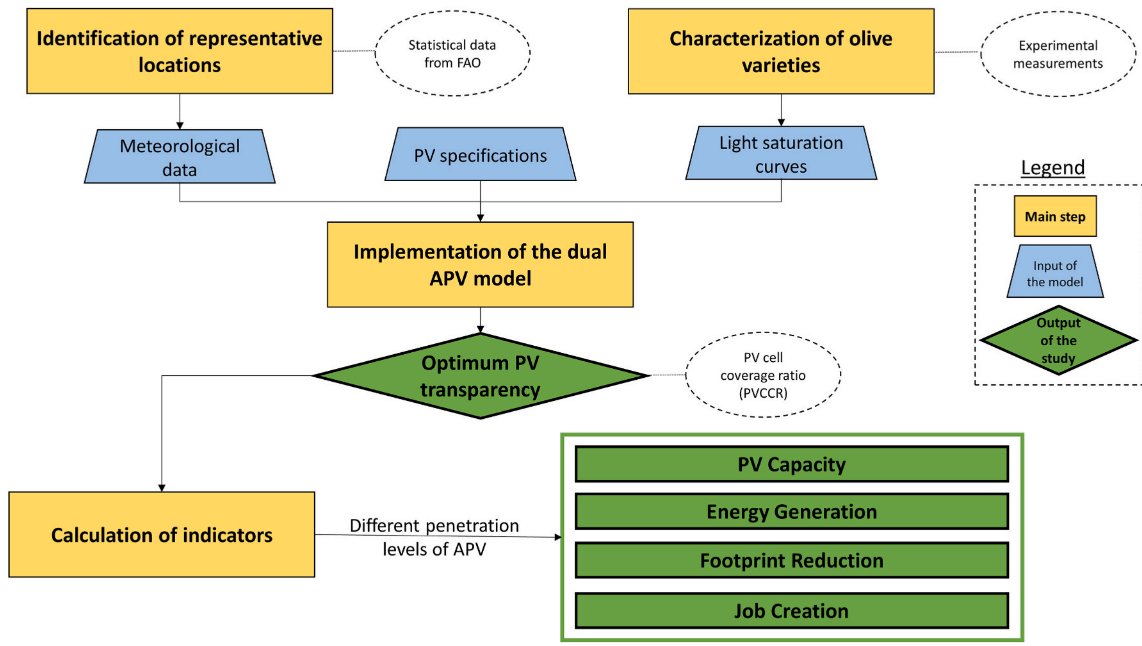

Fig. 2. Methodology and flowchart of the study.

United Nations (FAO) [43]. The second stage consisted in the selection of representative sites in each country. The olive farming does not tend to be uniformly distributed across the surface of the distinct countries, as in each one, there are usually regions where both the climate and the soil properties fit better to olive farming. The main environmental factors that impact the olive growth are the temperature and the precipitation. The ideal conditions for olive tree cultivation are characterized by warm to hot, dry summers and mild wet winters, which are typical of the Mediterranean climate [44]. Extreme temperatures ($>$ 40 °C in summer and $< -$ 8 °C in winter) negatively affect the crop yield, and especially, the occurrence of frost linked to the coldest ones during periods of more than one week can be lethal to olive trees [45]. The second climatic factor is precipitation despite the fact that nowadays ~90% of the olive groves in Mediterranean countries are periodically irrigated through pipes [46]. However, precipitations are strongly linked to the soil properties, which also play a key role in the development of olive trees. In spite of the ability of these trees to be adapted to low-fertile and poor soils, deep ones with a moderate water holding capacity represent the best option for their appropriate growth [47].

Bearing the above in mind, in the second stage, the characteristic olive cultivation sites in each country have been selected by using the data from the maps published by Caudullo et al. [48] and the information gathered from both governmental websites and specialized agricultural webpages. Table 1 summarizes the locations evaluated in this work. The coordinates of the sites are used to download meteorological data (solar irradiance and temperature) from PVGIS [49].

2.2. Characterization of olive varieties

The characteristics of three different cultivars of the Olea europea L. (*Picual*, *Manzanilla* and *Chemlali*) have been employed in this study. These cultivars are samples certified by the World Olive Germplasm Bank of Córdoba (Spain) and were selected according to two main criteria: (i) they are predominant varieties in some of the selected locations, and (ii) there are significant differences in their light-response curves between them. Below, we indicate some of the main properties of the evaluated cultivars. Picual produces >50% of the Spanish olive oil [59]. In addition, it has excellent organoleptic characteristics and it is one of the most profitable olive varieties with an intermediate seed vigor. In a conventional olive grove, olive trees of this variety can reach heights up to 5 m. However, they can adapt to super-intensive cultivation if regular pruning is conducted. Manzanilla de Sevilla is the most

Table 1
Selected countries and locations with the total olive groves area and the GPS coordinates used in the simulations. The annual average temperature and the annual horizontal global radiation values calculated from TMY data, which were downloaded from PVGIS, are also shown.

Country	Area (ha)	Location	GPS coordinates (latitude; longitude)	Annual average temperature (°C)	Annual horizontal global radiation (kWh/m^2)	Reference
Spain	2,750,000[a]	Jaén	37.77; −3.79	16.3	1883	[50]
Italy	1,157,000[b]	Apulia	41.00; 16.00	14.9	1574	[51]
Tunisia	1,800,000[c]	Sfax	34.74; 10.76	20.5	1941	[52]
Morocco	1,104,000[d]	Meknès	33.89; −5.55	18.1	1980	[53]
Türkiye	889,000[d]	Izmir	38.42; 27.14	17.6	1869	[54]
Algeria	440,000[d]	Setif	35.82; 5.51	14.0	1873	[55]
Egypt	101,000[d]	Al Jizah	30.01; 31.21	22.3	2220	[56]
Greece	819,000[d]	Peloponnese	37.36; 22.35	14.0	1688	[57]
Portugal	380,000[d]	Alentejo	38.57; −7.90	16.3	1830	[58]

[a] Ministerio de Agricultura, Pesca y Alimentación. Gobierno de España. https://www.mapa.gob.es/es/agricultura/temas/producciones-agricolas/aceite-oliva-y-aceituna-mesa/aceite.aspx.
[b] Istat Statistics. https://www.istat.it/it/agricoltura?dati.
[c] Ministère de l'Agriculture, des ressources hydrauliques et de la pêche. https://www.onh.com.tn/.
[d] FAOstat. https://www.fao.org/faostat/en/#data/QCL.

important table olive variety. It is widely cultivated both in Spain [59] and in other countries (Argentina, Australia, south-west of United States (Manzanillo Olive), Israel and Portugal). It is a low-vigor variety that easily adapts to super-intensive cultivation, as it can reach a maximum height of 3.5 m if no pruning is performed. Chemlali Sfax cultivar is the most abundant variety in Tunisia [60]. It has been chosen for its great ability to adapt to drought. It is a tree of great vigor and it can reach a large size, with a typical height of 8 m if not pruned.

Next, we explain the methodology that we employed to characterize the three different olive cultivars. First, one-year-old plants were grown in a culture chamber, irrigated ad libitum and kept at constant ambient conditions (40% of relative humidity, 21 °C of temperature). Throughout the experiments, they were consistently exposed to a fixed daily photoperiod, which consisted of 16 h of light and 8 h of darkness. Six specimens of each cultivar were used to measure the photosynthetic curves. The measurements were conducted five times to ensure the repeatability of the results.

The photoresponse curves of the leaves were measured using a LI-Cor 6800 photosynthetic analyzer. Firstly, before making the measurements, the plants were adapted to the darkness during the previous day. Then, saturated pulsed light (3000 μmol m^{-2} s^{-1}, 300 ms duration) was applied to determine the minimal (F_0) and maximal chlorophyll fluorescence (F_m) of plants when all photosystem II (PSII) reaction centers were open and closed after dark acclimation, respectively. Next, when the plants were light-adapted, the minimal (F_0') and the maximal fluorescence (F_m') were determined in those conditions. Subsequently, by using these data, photosynthetic-light curves were measured. During the measurements, the following parameters were set and controlled in the analyzer: CO_2 concentration of 400 ppm, relative humidity of 40%, ambient temperature of 21 °C, flow of 500 mmol s^{-1}, fan speed of 10,000 rpm and color spectrum of the light (R90 B10). The light intensity gradient of the photoresponse curves was: [0, 50, 100, 150, 250, 500, 1000, 1500, and 2000] μmol m^{-2} s^{-1} with minimum and maximum wait times of 60 s and 180 s, respectively, between the different photosynthetic photon flux density (PPFD) values. The choice of this gradient allows an accurate modeling of the relationship between the PPFD and the net photosynthesis rate (PSN) in μmol (CO_2)/m^2s. This relation is obtained by following the same method explained in [25], in which the experimental measured data were fitted to a fourth-order degree polynomial. Fig. 3 shows the photosynthetic light-response curves of the three olive varieties evaluated in this work.

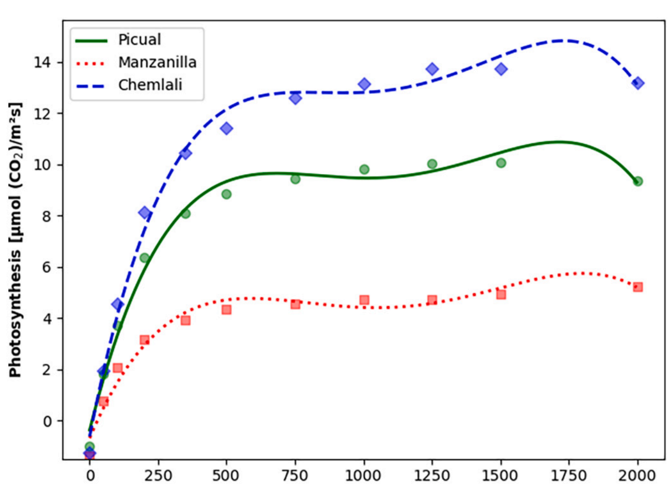

Fig. 3. Photosynthetic light-response curves of the three olive cultivars under study. The different markers (circle – Picual, square – Manzanilla, and diamond – Chemlali) represent the experimental measurements and the lines represent the fit of the data with a fourth-order degree polynomial.

2.3. APV configuration

In this subsection, we introduce a practical setup for an APV system in the context of olive cultivation. Recent reports have highlighted the growing significance of super-intensive olive farming, particularly in the Iberian peninsula [61–63]. Therefore, our study suggests a PV system design suitable for such olive groves, which are characterized by a high density planting pattern (>1600 olive trees/ha) [64]. Additionally, in this cultivation method, the size of the olive trees is controlled by regular pruning, maintaining them at typical dimensions of 2 m in height and 0.8 m in width. It should be noted that both Manzanilla and Picual are olive cultivars that readily lend themselves to the super-intensive farming method. Also, in this approach, the trees are typically planted with a spacing of 1.5 × 3.5 m as depicted in Fig. 4.

The illustrated PV system layout is also presented in Fig. 4. The modules are strategically placed on an elevated canopy, situated 4 m above the ground, and oriented towards the south with a tilt angle of 30° in landscape configuration. To prevent shading between the modules, they are installed with a row spacing of 1.7 m. This distance has been calculated by considering the dimensions of the modules and by using the equations indicated by Swaid et al. [65]. This particular design allows the harvesting machine, which can have a maximum height of 3.5 m height, to pass over the olive trees. The tilt angle of the modules can contribute to mitigate the energy losses caused by soiling [66]. Based on the provided layout, the ground coverage ratio (GCR), which represents the ratio of the PV modules area to the total ground area, is 0.5. It should also be noted that the same configuration is applied across all the sites, ensuring that the GCR remains consistent regardless of the location.

2.4. Dual APV model

This study aims to calculate the suitable level of transparency that PV modules placed above olive trees should have to avoid a risky decrease of the total CO_2 assimilated during the photosynthesis, and, thus, preventing a likely reduction in the olive yield. In this subsection, the assumptions and approximations that have been considered, the methodology, and the criterion that has been followed to solve the problem are detailed.

2.4.1. PV module transparency

In the dual APV model presented here, the semi-transparent PV modules consist of a combination of transparent and active areas, as it is shown in Fig. 5. This leads to the definition of two different indexes, presented for the first time in [25]. The photovoltaic active factor (PVF) represents the relationship between the PV active area and the total area of a module. It can be calculated by using Eq. (1):

$$PVF = \frac{A_{active}}{A_{total}} = \frac{A_{active}}{A_{active} + A_{glass}} \tag{1}$$

Also, to calculate the transmittance of a semi-transparent PV module for a certain wavelength (λ) with the configuration shown in Fig. 5a, an indicator, named transmittance factor (TRF) is defined. This considers both the transmittance of the transparent area, which is typically glass, and the transmittance of the active part. The TRF can be obtained through the following equation:

$$TRF\ (\lambda) = \tau_{glass}(\lambda) \bullet (1 - PVF) + \tau_{active}(\lambda) \bullet PVF \tag{2}$$

In this work, opaque m-Si PV cells are considered, so the transmittance of the active part is 0. Also, as the photosynthesis occurs within the wavelength range 400–700 nm [67], and in this region, the transmittance of a PV glass remains almost constant (see Fig. 5b), the global transparency of a semi-transparent PV module for APV purposes can be calculated by using Eq. (3):

$$TRF = \tau_{glass} \bullet (1 - PVF) \tag{3}$$

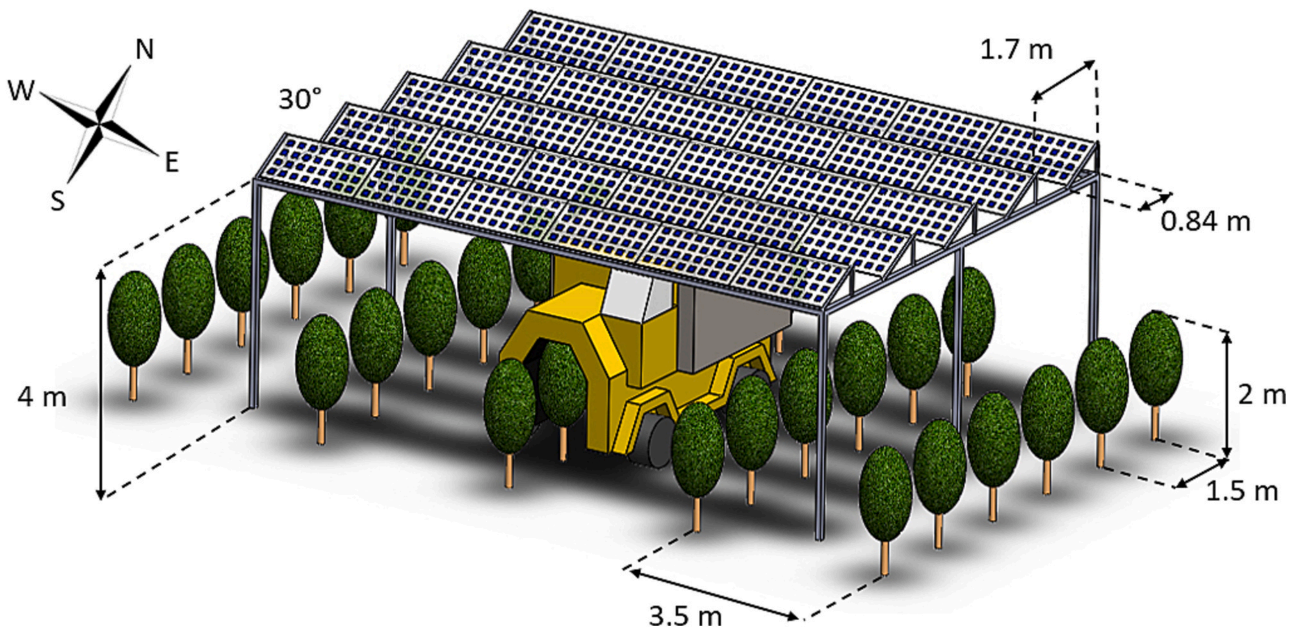

Fig. 4. APV system configuration. Fixed-tilt PV modules are positioned facing due south and installed above a super-intensive olive grove. The olive grove features a high planting density with a distance of 3.5 m between rows of trees and 1.5 m between individual trees.

a)

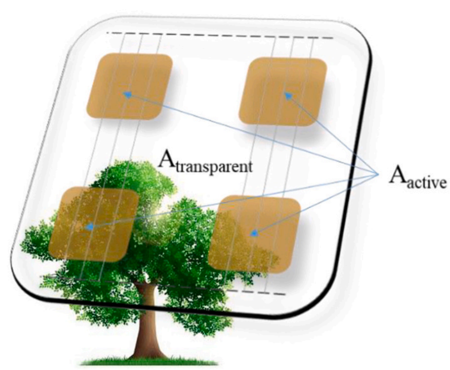

b)

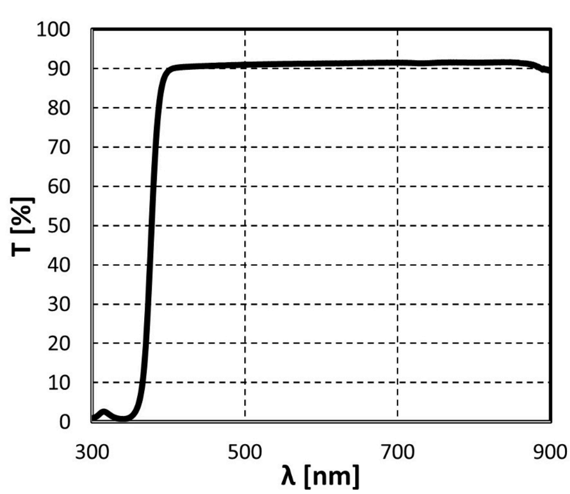

Fig. 5. a) Schematic of a semi-transparent PV module, and b) transmittance profile of a typical PV glass.

The glass transmittance (τ_{glass}) used in this study is 0.90, which is in line with the transmittance profile of a low-iron glass sample shown in Fig. 5b, and which was also measured in a global PV soiling research [68].

2.4.2. Model inputs and main equations

The model uses as inputs hourly meteorological data, PV specifications and the photosynthetic light-response curves of the different olive varieties. Typical meteorological year (TMY) data are downloaded from PVGIS, which provides datasets with 1-h resolution, for each of the selected locations. The meteorological parameters of interest for the model are the different broadband horizontal irradiance components, the direct normal irradiance and the air temperature. Then, the plane-of-array irradiance (G_{POA}) is calculated by using the *get_total_irradiance* function in the pvlib library for Python 3.7 [69]. For the sake of simplicity, for all the sites, the same azimuth (180° - South) and tilt angle (30°) values have been introduced as inputs. Another inputs of the function that should be mentioned are: the use of the isotropic sky diffuse model [70] to calculate the POA sky diffuse irradiance and the albedo coefficient, which has been set to 0.309, using as reference the leaf reflectance of olive varieties presented in [71]. The output of this function, which is the POA irradiance, is then used to calculate the PV power generation.

In addition, the spectral irradiance components (G_{POA}, direct horizontal and diffuse horizontal) are also modeled with 1-h resolution for the different sites by using the Bird Simple Spectral Model (SPECTRL2) [72] implemented in the *spectrum.spectrl2* function in the pvlib library for Python 3.7. This model returns solar spectra under clear-sky conditions, so, then the outputs should be scaled to match the broadband components obtained from the TMY. The same procedure as in [25] has been followed to do this. The use of the spectral irradiance is accounted for the need to accurately calculate the photosynthetically active radiation (PAR), which represents the solar radiation within the wavelength range 400–700 nm, as it was abovementioned.

Once the broadband G_{POA} and the spectral irradiance components have been obtained, the next step of the model is the calculation of the power per unit area of PV modules (P/A) in W/m^2 by using Eq. (4):

$$P/_{A} = G_{POA} \bullet \eta_{PV,STC} \bullet PVF \bullet AOIF \bullet SF \bullet TF \quad (4)$$

where $\eta_{PV,STC}$ is the PV cell efficiency under Standard Test Conditions (STC) (1000 W/m^2, AM1.5G spectrum and Tc = 25 °C), and AOIF, SF and TF are the angle-of-incidence factor, the spectral factor and the thermal factor, respectively. These three factors are utilized to correct the power when the conditions differ from the STC. A $\eta_{PV,STC}$ value of 0.20 has been used in this study, as this is a typical efficiency value of commercially available crystalline silicon modules. A detailed explanation of the correction factors can be found in [25]. The PV energy per unit area in kWh/m^2 generated over a specific time interval can be calculated by integrating the time series results provided by Eq. (4). This value is also one of the two main outputs of the dual APV model.

The other main output of the model is the total amount of CO_2 assimilated by the crop during the photosynthesis over a time interval. This is achieved through a four-step process. First, the spectral irradiance that falls on the olive tree is calculated by using Eq. (5). It is assumed that there is a uniform light distribution on the tree leaves [25].

$$E_{plant}(\lambda) = \left[E_{DH}(\lambda) \bullet AOIF + E_{DiffH}(\lambda)\right] \bullet TRF(\lambda) \tag{5}$$

where E_{DH} and E_{DiffH} are the direct horizontal and the diffuse horizontal spectral irradiance, respectively.

Then, the PAR, in μmol /(m^{2}s), is obtained by using the following expression:

$$PAR = \int_{400}^{700} \frac{E_{plant}(\lambda) \bullet \lambda}{N_A \bullet h \bullet c} d\lambda \tag{6}$$

where N_A is the Avogadro's constant, h is the Planck's constant and c is the speed of light constant.

Next, and due to the particular spectral distribution of the instrument used to measure the light-response curve of the leaves, which does not match the actual irradiance that falls on the trees, a mismatch spectral factor is required to correct the PAR radiation. This mismatch factor considers both the spectral irradiance of the instrument and the actual one, and the quantum yield of the crops. Additional information about the computation of this mismatch factor can be read in [25]. Last, by using the fourth-order degree polynomial mentioned in Section 2.2, the PSN is obtained. The CO_2 uptake during a specific time interval can be calculated by integrating the PSN over time.

The criteria, which have been used in this study to estimate the transparency that PV modules placed above different olive tree cultivars should have, are detailed in Section 3.

2.5. Calculation of indicators of APV potential

To assess the potential of APV systems into olive groves in the Mediterranean region, different indicators have been calculated in this work. The first step has been the identification of the surface occupied by olive trees in the different selected countries. These values are shown in Table 1. Then, three different levels of penetration of APV into existing olive groves are proposed: high, medium and low, which consider that PV systems would be installed in 25%, 10% and 1% of the olive groves surface, respectively. Below, the distinct indicators are defined.

2.5.1. Installed PV capacity

The installed PV capacity is calculated by using the following equation:

$$PV\,capacity\,[kWp] = k_{PV} \bullet PVF_i \bullet GCR \bullet Land\,Surface\,\left[m^2\right] \bullet 200\frac{Wp}{m^2} \bullet \frac{1}{1000} \tag{7}$$

where k_{PV} is a constant that represents the level of penetration (0.25 for a high penetration, 0.10 for a medium penetration and 0.01 for a low penetration), PVF_i is the suitable PVF value for each location calculated according the annual criterion, and GCR is the ground coverage ratio, which has a value of 0.5 independently of the location, as commented in Section 2.3. The value of 200 Wp/m^2 is accounted for the choice of PV modules with a 20% efficiency.

2.5.2. Energy generation

The potential annual energy that can be produced by APV systems into olive groves is obtained by means of the following expression:

$$PV\,energy\left[\frac{kWh}{year}\right] = k_{PV} \bullet PVF_i \bullet GCR \bullet Land\,Surface\,\left[m^2\right] \bullet E_{PV}\left[\frac{kWh}{m^2 \bullet year}\right] \tag{8}$$

where E_{PV} is the generated energy per unit area of PV modules, which is also one of the outputs of the APV model.

2.5.3. Reduction in CO_2 emissions

According to the current policies towards the decarbonization of the energy system, the estimation of the avoided emissions of CO_2 due to the potential implementation of APV systems is essential. This is done by using Eq. (9).

$$Reduction\ in\ CO_2\left[\frac{kg}{year}\right] = PV\ energy\left[\frac{kWh}{year}\right] \bullet k_{CO_2}\left[\frac{kg\ CO_2}{kWh}\right] \tag{9}$$

where k_{CO2} represents the CO_2 emission coefficient, in kg (CO_2)/kWh. This coefficient indicates the average CO_2 emissions per kWh of energy supply, and it depends on the energy mix of each country. The coefficient values have been extracted from the "Greenhouse Gas Emissions from Energy" report published by the International Energy Agency [73]. It is important to note that the calculations presented in this analysis are based on the assumption that it is feasible to either consume or store all of the energy generated.

2.5.4. Job creation

The generation of new employments due to the installation of new PV systems is one of the aspects that contributes to favoring the social acceptance of the implementation of this kind of systems in certain areas [39]. For this reason, it is important to estimate the amount of potential jobs that would be linked to both the construction and installation, and the operation and maintenance of PV systems integrated within olive groves. The number of new jobs can be estimated by using the following equation:

$$Job\ creation_{i,c} = PV\ capacity\ [MWp] \bullet EF_i\left[\frac{jobs}{MW}\right] \bullet REM_c \tag{10}$$

where EF represents the employment factor and the subindex i indicates the purpose of the jobs that would be created. The purposes can be the construction and installation (C&I) or the operation and maintenance (O&M) of the PV systems. For C&I, the employment factor equals to 13 jobs/MW and for O&M, its value is 0.7 jobs/MW [74]. The regional employment multiplier (REM) is a parameter that incorporates the variations in labor-intensive economic activities across different regions worldwide. The value of REM is normalized for countries belonging to the Organization for Economic Cooperation and Development (OECD), as presented by Ram et al. [74]. In general, countries with lower labor costs tend to employ a larger number of workers to produce the same unit of output. It should be noted that over time, the REM values are expected to undergo changes, corresponding to the evolving differences in labor productivity that accompany regional economic growth. In our analysis, we consider the specific REM values to the year 2025 mentioned in [74], which are 1 for OECD countries (Spain, Italy, Greece, Türkiye and Portugal) and 1.66 for the countries located in the MENA region (Morocco, Algeria, Tunisia and Egypt).

3. Evaluation of the PV transparency

The implementation of APV systems to mitigate land-use conflicts should consider a wide range of factors. Among these, the assessment of the shading caused by the PV modules on the crops is one of the most relevant, as it may negatively affect the photosynthesis process. Herein, the evaluation of the transparency levels of PV modules is conducted. In this work, the criterion that has been followed to get these values was previously employed by Fernández et al. [25]. They indicated that a 10% decrease in the overall yearly photosynthesis would not significantly impact the growth of the crops and, consequently, the final crop yield. In addition, a variation of the original approach has also been considered. This latter does not consider the winter months in the calculations, as during the winter and once the fruits have ripened, the tree reduces its photosynthetic activity and its buds become dormant to minimize the damage that tissues may experience because of the cold temperatures. This activity regains its maximum intensity when the tree detects an increase in temperatures. To find the most suitable PV transparency, a sensitivity analysis is done by varying the PVF from 0 (all the PV module area is active area) to 1 (there is only glass area) with a step of 0.05 for each site and olive cultivar under study. Fig. 6 represents the simulation result considering the original criterion for the location in Spain and the Picual cultivar. The simulated suitable PVF is 0.36, which directly translates into a transparency factor of 0.64.

Fig. 7-left displays the results of the PV transparency for the different sites and cultivars. The values of the transparency factor vary between 0.57 (Egypt & Manzanilla) and 0.71 (Italy & Chemlali). Also, it can be appreciated that Chemlali is the analyzed cultivar that requires more sunlight as higher transparency factors ($>$ 0.65) are obtained. Consequently, this leads to a reduction in the active area available per PV module. Almost identical results are returned for the other two varieties, Manzanilla and Picual, with slightly higher transparency values for Picual in most of the sites. In the right plot of Fig. 7, the average transparency values for the different countries are represented. A correlation between the total annual radiation and the transparency factor was found: the higher the solar radiation the lower the PV transparency. This can be noticed by the analysis of different locations. For example, the sites in Egypt and Tunisia, which present the greatest solar radiation with 2390 kWh/m^2 year and 2140 kWh/m^2 year, respectively, and the lowest average transparency factors: 0.60 and 0.63, respectively. At the other end of the spectrum, the Italian site, with ~1735 kWh/m^2 year, needs the highest transparency, with an average of 0.69 for the analyzed olive varieties.

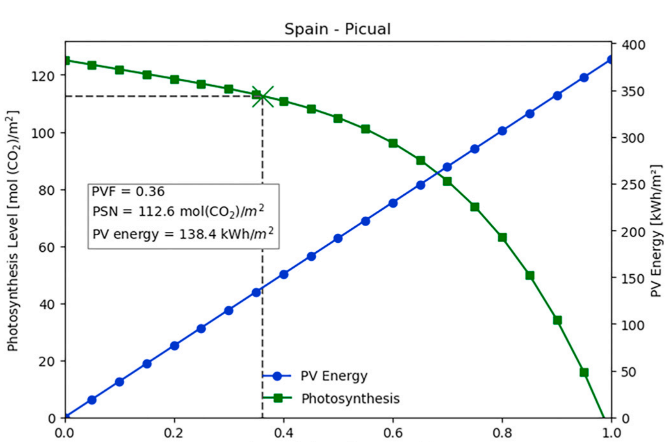

Fig. 6. Simulation of the most suitable PV transparency for the site in Spain and Picual cultivar considering the criterion of the 10% drop in the accumulated annual PSN.

Fig. 8 shows the annual PV energy generation per m^2 of ground that can be obtained in the different sites without causing a detrimental impact on the olive production. The results have been calculated by considering the PVF values estimated before and the PV configuration detailed in Section 2. We have used the average value of the PVF for the three different olive cultivars under evaluation. Again and as expected, there is a relationship between the amount of solar radiation and the energy generation. The highest value is 83.7 kWh/m^2 (Egypt) and the lowest one is 48.9 kWh/m^2 (Italy), whereas the average is 65.9 kWh/m^2.

As it was mentioned before, the calculation of the suitable PV transparency is also done by removing the data from the winter months (December, January and February) from the analysis, i.e. only meteorological data from the months when the olive growth cycle occurs are utilized. This approach aims to maximize the PVF, resulting in a higher energy generation per unit area, without affecting the olive yield. Fig. 9 represents the increase in PVF when considering only the months associated with the olive growth cycle. The largest increase, amounting to 3.5%, is observed for the Italian site. Conversely, the impact on PVF is minimal ($<$ 0.2%) in Egypt. These results can be explained by the distribution of solar radiation throughout the year. In regions where the contribution of radiation during the winter months is relatively low ($<$ 15%), excluding these months from the calculation leads to a more significant increase in PVF (e.g., Italy, Greece, and Turkey). On the other hand, in Egypt, where the total accumulated radiation is evenly spread throughout the year, the increase in PVF is marginal.

4. Assessment of the potential of APV into olive groves

In this section, an in-depth discussion on the potential of APV systems into olive groves in the Mediterranean region is included. As it was abovementioned, three different penetration scenarios of this technology into olive cultivation are considered. Notwithstanding the foregoing, the current status of PV installations, e.g. installed PV capacity, is also taken into account to analyze the distinct scenarios. The indicators are calculated using the transparency factors depicted in Fig. 7b, which have been derived based on the original criterion. This considers a maximum drop of 10% in the accumulated annual PSN, which includes the winter months in the calculations.

Fig. 10 shows the PV capacity additions in the different countries according to the distinct scenarios. As it was mentioned before in Section 2.5, we evaluate three different levels of APV system integration in olive groves: (a) High penetration, which involves installing PV systems on 25% of the entire olive grove area, (b) Medium penetration, where PV systems cover 10%, and (c) Low scenario, with PV systems on only 1% of the olive grove area. These penetration levels can be achieved in the near to medium term, considering the proposed APV configuration in Section 2.3. This configuration specifically targets super-intensive olive cultivation areas, which are increasingly being adopted worldwide. Experts predict that by 2030, >20% of olive production will be accomplished using the super-intensive approach [75,76]. In the High penetration scenario, notable figures such as 243 GWp in Spain or 168 GWp in Tunisia are observed when compared to the current global PV capacity, which has just exceeded the 1 TWp threshold in May 2022 [77]. Similarly, but in a lower magnitude, the Medium scenario also provides very high values. These are ~100 GWp in Spain and ~ 70 GWp Tunisia, and over 10 GWp in the other countries, with the exception of Egypt (4 GWp). These results highlight the vast potential of APV into olive groves. In the Low scenario, there are still large values in those countries with greater land surface occupied by olive trees. For example, in Spain, the conversion of 27,500 ha (1% of the total olive-growing area), which are currently dedicated to super-intense olive cultivation, into APV systems would mean the addition of 9.7 GWp of PV. This would correspond to a significant 46% increase in the country's installed PV capacity [78].

The PV energy generation in the different scenarios along with the data of electricity demand in each country in 2021 are represented in

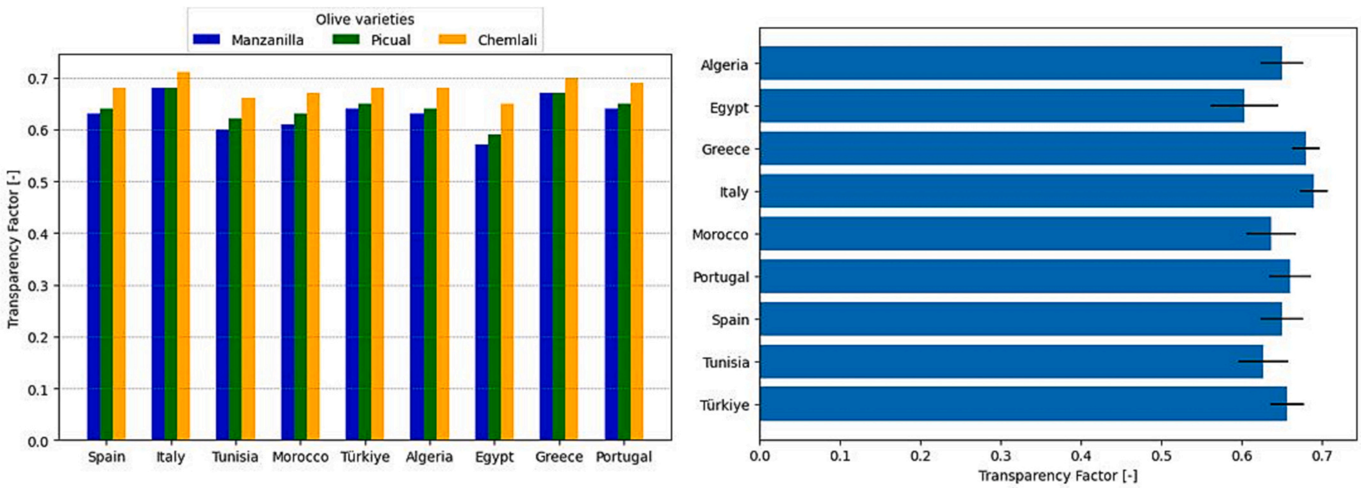

Fig. 7. Left – Annual suitable PV transparency for the different sites and olive varieties. Right – Mean annual suitable PV transparency for the three evaluated olive varieties. The black lines represent the standard deviation.

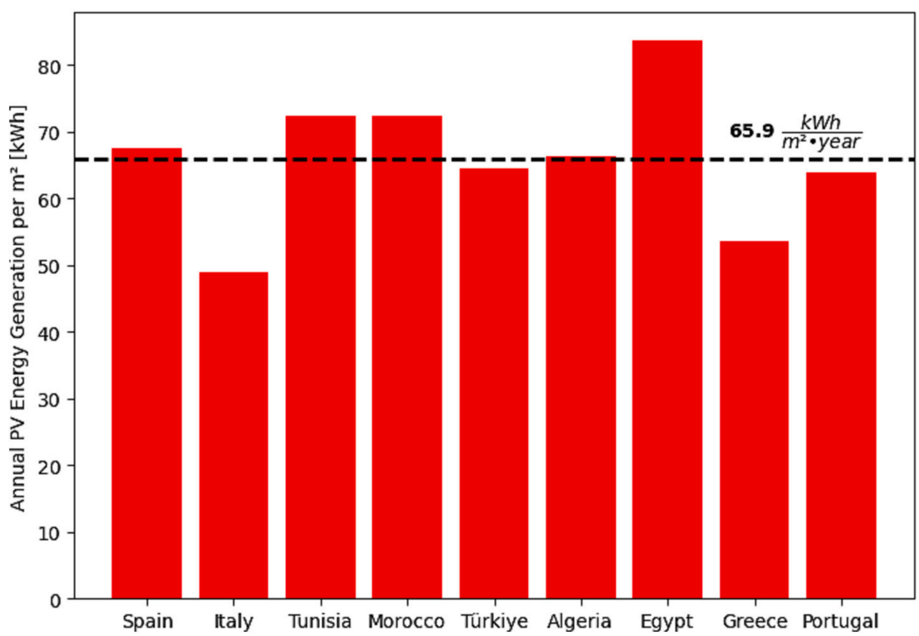

Fig. 8. Annual PV energy generation per unit area according to the suitable PVF in each location (suitable PVF = 1 – Transparency Factor (shown in Fig. 7-Right)). The horizontal dashed line represents the average value for the set of locations under study.

Fig. 11. In the High scenario, the expected PV generated energy would allow to satisfy the electricity demand in two countries: Tunisia and Morocco. In Spain, which is the third country with the greatest demand (234 TWh in 2021) among the evaluated ones, 164 TWh/year could be generated. In the Medium scenario, the Tunisian electricity demand could be still covered just with APV systems into 10% of the olive groves surface. The Low scenario, which is defined by the conversion of 1% of the olive-growing area into APV installations, would imply levels of electricity demand coverage between 0.2% (Egypt) and 30.3% (Tunisia). Although these results can be seen as low when compared with the other two scenarios, the values should be put in context. As an example, in Spain and considering the Low scenario, 6.6 TWh, which represent a 2.8% of the 2021 electricity demand, would be produced. However, it is noteworthy that this amount of energy represents a significant proportion, specifically 23.3% of the energy generated by grid-connected PV installations in 2022 [79].

The displayed figures in Figs. 10 and 11 underline the massive potential of APV into olive groves. Hereon, the following indicators related to the reduction of CO_2 emissions and job creation are only evaluated under the hypothesis of the Low scenario. This decision can be justified by the goals that are nowadays being proposed related to renewable energy generation at European and national scales. The target proposed by the European Commission in the REPowerEU Plan related to solar PV contemplates the addition of 600 GWp of new installations by 2030 [81]. In Spain, the renewable generation is expected to cover 74% of the total energy production in 2030. To achieve this level, the solar PV capacity should be ~37 GW by that date [82], indicating the need for 17 GW of new installations. These latest values of PV capacity additions are in line with the Low scenario, which indicates a total addition of 32.9 GW in the evaluated Mediterranean countries and 9.7 GW in Spain due to the installation of APV systems over olive groves.

In the 2030 Climate target plan proposed in the context of the

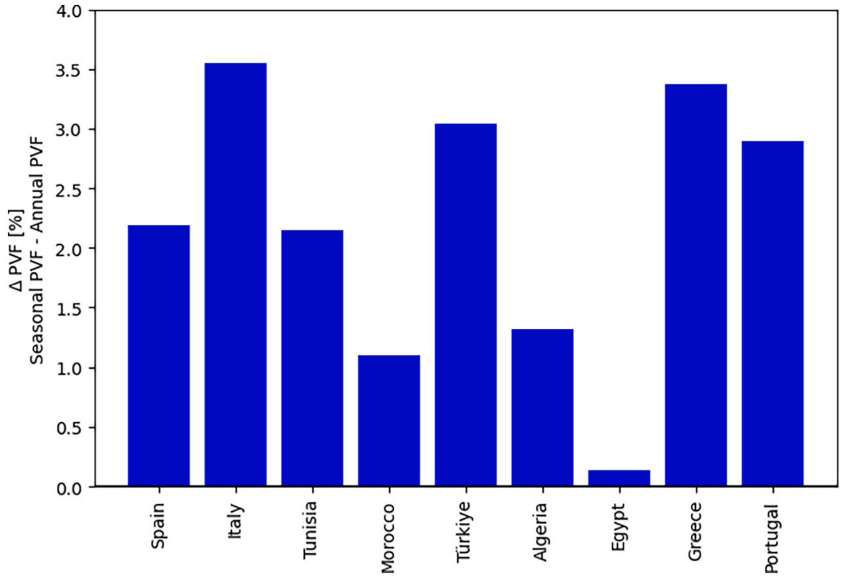

Fig. 9. Change in the Photovoltaic Active Factor (PVF) when only data from the months in which the olive growth cycle occurs are included in the calculations.

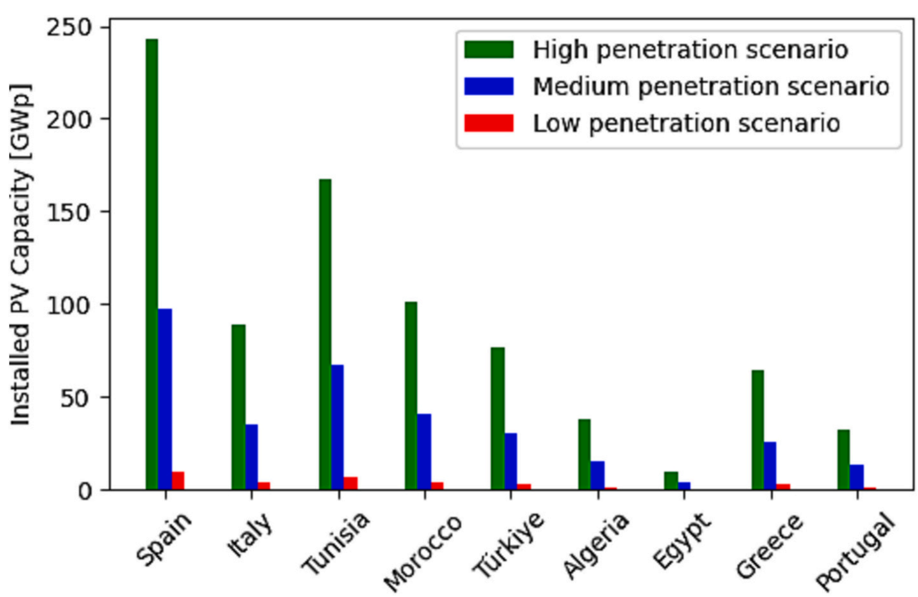

Fig. 10. Installed PV capacity in different countries located in the Mediterranean region based on different scenarios of APV penetration into olive groves. The high, medium and low scenarios contemplate that the 25%, 10% and 1% of the olive groves surface would be occupied by APV systems.

European Green Deal [83], one of the targets is to cut greenhouse gas (GHG) emissions by a minimum of 55% by 2030 considering as reference the emissions in 1990. In this study, the same goal has been expanded to the different evaluated countries in the Mediterranean region. Fig. 12 shows the coverage of the target based on the conversion of 1% of the olive groves area into APV installations along the required amount of CO_2 reduction to meet it. The best results correspond to Tunisia and Greece, where 3.9% and 1.6% of the target could be covered, respectively. In the case of Tunisia, this result is due to a conjunction of two factors: the large amount of area occupied by olive groves (1.8 million of ha) and the low amount of CO_2 emissions that should be avoided (25.2 Mt./year). In Greece, the high coverage is mainly justified by the current status of the target, as in 2021, the CO_2 emissions were already 33% lower than the ones registered in 1990. Other countries that would register coverage levels above the 0.5% threshold are Spain, Morocco and Portugal. On the other hand, in Egypt, the implementation of APV systems based on the Low scenario would only mean a 0.03% coverage of the target. This can be explained by the relatively low surface of olive groves (~100,000 ha) and the high absolute value of the 55-CO_2 reduction target, which is the second largest among the analyzed countries.

Finally, it should be mentioned that the conversion of purely olive groves into APV systems has the potential to generate significant job opportunities. These jobs can be classified into two main categories: construction and installation (C&I) of the PV system, and operation and maintenance (O&M) tasks.

Fig. 13 provides an overview of the potential job creation resulting from the conversion of 1% of the olive grove surface into APV systems. The countries with larger olive-growing areas, such as Spain and Tunisia, are expected to experience the highest job generation. In terms of C&I jobs, Tunisia shows the highest potential, with an estimated creation of 144,664 jobs. On the other hand, Egypt has a comparatively lower job creation potential in this category, with an estimate of 8628 jobs. When it comes to O&M tasks, Tunisia again leads with an estimated

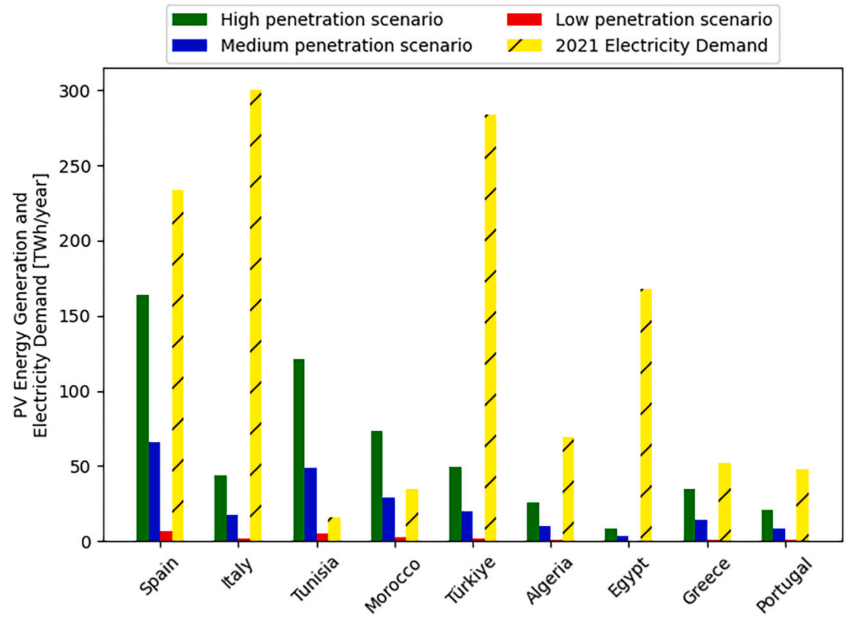

Fig. 11. PV energy generation (colored bars) based on the different scenarios of APV penetration into olive groves and 2021 electricity demand (dashed yellow bars) in the different countries. The electricity demand data have been sourced from the US energy information administration [80]. (For interpretation of the references to color in this figure legend, the reader is referred to the web version of this article.)

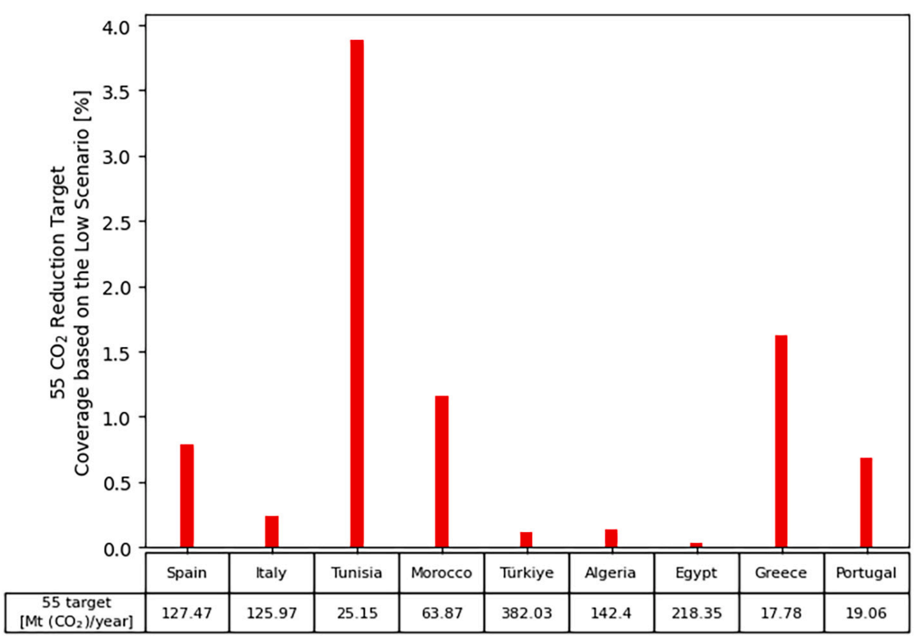

Fig. 12. Potential of APV into olive groves to meet the 55-CO_2 reduction target. The bars represent the relative coverage of the 55-CO_2 reduction target proposed by the European Union in the different countries based on the Low scenario (1% of the national olive-growing area converted into APV systems). The values below the plot represent the amount of CO_2 per year that should be avoided to meet the 55 target. These have been calculated from [84].

requirement of 7790 jobs, followed by Spain with 6792 jobs.

Overall, the conversion of olive groves into APV systems can lead to the creation of substantial employment opportunities in the Mediterranean region. Across the nine evaluated countries, >560,000 jobs could be generated, contributing to local economies and addressing unemployment challenges.

This evaluation highlights the potential benefits of transitioning to APV systems, not only in terms of renewable energy generation, but also in terms of stimulating economic growth and creating employment opportunities within the olive-growing sector.

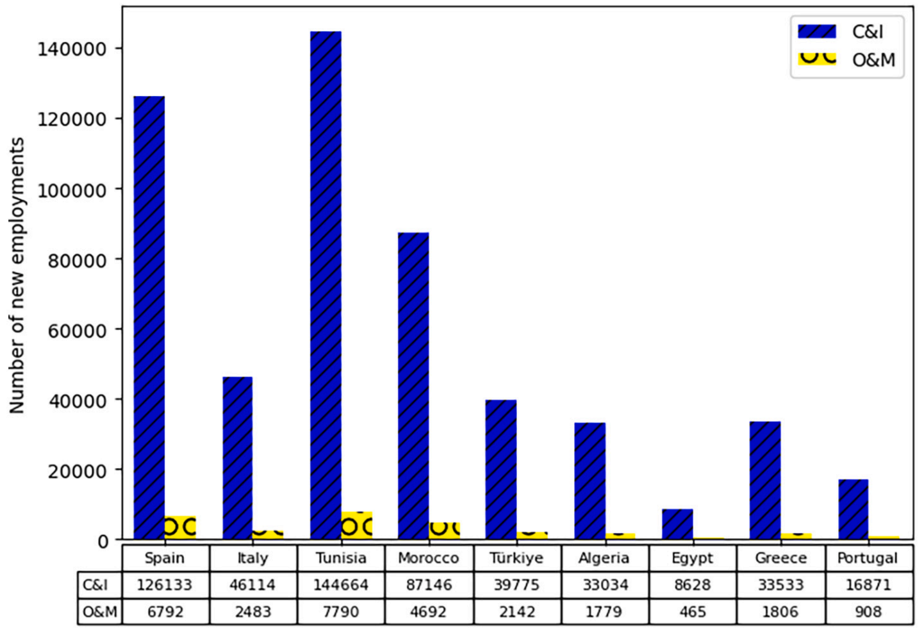

Fig. 13. Potential creation of new jobs based on the conversion of 1% of the olive groves surface into APV systems. Two different categories: C&I stands for the construction and installation of the PV system, and O&M stands for the operation and maintenance tasks in the commissioned systems.

5. Conclusions

This study evaluates the potential of the integration of agrivoltaics (APV) systems into existing olive groves in the Mediterranean area. The suitable transparency levels of PV modules placed above three different olive cultivars (Manzanilla, Picual and Chemlali) have been calculated for nine representative olive cultivation locations. The potential assessment of these kind of agrivoltaics system into olive groves has been conducted by analyzing different indicators, such as the PV capacity, the energy generation, the avoided CO_2 emissions and the job creation.

The suitable transparency factors that have been obtained using the annual criterion fluctuate between 0.57 and 0.71. Lower values are returned for those locations with higher solar irradiation, such as Egypt and Tunisia. Another finding is that the Chemlali cultivar is the one that requires more sunlight, as the greatest transparency factors correspond to this variety in all the locations. It has been also evaluated the impact of removing the winter months from the procedure according to the phenological phases of the olive trees, finding that in those locations where the incident solar radiation in winter is lower, such as the Italian location where only 13.2% of the total annual radiation falls during the winter, the appropriate transparency decreases more compared to the annual and to other sites with a more uniform radiation distribution throughout the year, such as Egypt or Morocco. This directly translates into an increase in the PV capacity that can be installed, with values >3.5% in Italy and <1% in Egypt.

With regard to the potential of APV systems into olive groves, the findings emphasize that even the integration of these systems into a modest fraction (1%) of the overall olive-growing area in each country would yield significant socio-economic advantages. In Spain specifically, the adoption of these systems would result in a nearly 50% surge in the country's installed national PV capacity. In Tunisia, the energy produced by these systems could cover 30.3% of the electricity demand. Also, these solutions would contribute to the CO_2 emissions reduction targets. In Tunisia and Greece, they would suppose a coverage of the 55-target >1.5%. Regarding job creation, >560,000 new employments would be generated in the nine countries of the Mediterranean region. It is important to note that future research should address several challenges, such as the effective consumption of the generated energy and the use of storage systems, to ensure the successful implementation of large-scale APV systems across different countries.

In future studies, more olive varieties should be analyzed to better customize the transparency factors for each situation. In addition, the utilized dual model should be improved by considering extra parameters, such as the influence of PV modules on the soil temperature and on the evotranspiration. Also, the social acceptance related to the installation of APV systems into olive groves should be carefully addressed to analyze the feasibility of these projects. Furthermore, and related to the aforementioned, an extension of this work will include a more exhaustive potential assessment by considering both geographical and legal constraints. Finally, future works should assess the impact of suppressing ultraviolet (UV) light on olive growth when PV modules are installed above olive trees, as the glass encapsulant absorbs this specific portion of the solar spectrum.

CRediT authorship contribution statement

Álvaro Fernández-Solas: Writing – review & editing, Writing – original draft, Visualization, Validation, Software, Methodology, Investigation, Formal analysis, Data curation. **Ana M. Fernández-Ocaña:** Writing – review & editing, Data curation. **Florencia Almonacid:** Writing – review & editing, Supervision, Project administration. **Eduardo F. Fernández:** Writing – review & editing, Supervision, Methodology, Investigation, Conceptualization.

Declaration of Competing Interest

The authors declare that they have no known competing financial interests or personal relationships that could have appeared to influence the work reported in this paper.

Data availability

Data will be made available on request.

Acknowledgements

Álvaro Fernández-Solas, the corresponding author of this work, is supported by the Spanish Ministry of Science, Innovation and Universities under the program "Ayudas para la Formación de Profesorado Universitario (FPU), 2018 (Ref. FPU18/01460)". Eduardo F. Fernández thanks the Spanish Ministry of Science, Innovation and Universities (RYC-2017-21910). This work is part of the "Greenhouse Living-lab Agrivoltaic Systems in Spain (GLASS)" (PLEC2022-009435) project funded by the Spanish Ministry of Science and Innovation. Part of this work was conducted as part of the project titled: "H2020 Gen4Olive Mobilization of Olive GenRes through pre-breeding activities to face the future challenges and development of an intelligent interface to ensure a friendly information availability for end users". Reference: 101000427 SFS-28-2018-2019-2020 Genetic resources and pre-breeding communities.

References

[1] United Nations. The sustainable development goals report 2022. 2022.
[2] International Energy Agency (IEA). Renewables 2022. Paris. 2022.
[3] De la Morena C. Las plantas fotovoltaicas, ¿energía limpia contra los pueblos?. 2022.
[4] Milman O. 'It's got nasty': the battle to build the US's biggest solar power farm. Guard 2022.
[5] Horton H. Ministers hope to ban solar projects from most English farms. Guard 2022.
[6] Adeh EH, Good SP, Calaf M, Higgins CW, Solar PV. Power potential is greatest over croplands. Sci Rep 2019;9:1–6. https://doi.org/10.1038/s41598-019-47803-3.
[7] Goetzberger A, Zastrow A. On the coexistence of solar-energy conversion and plant cultivation. Int J Sol Energy 1982;1:55–69. https://doi.org/10.1080/01425918208909875.
[8] Yano A, Cossu M. Energy sustainable greenhouse crop cultivation using photovoltaic technologies. Renew Sustain Energy Rev 2019;109:116–37. https://doi.org/10.1016/j.rser.2019.04.026.
[9] Elamri Y, Cheviron B, Mange A, Dejean C, Liron F, Belaud G. Rain concentration and sheltering effect of solar panels on cultivated plots. Hydrol Earth Syst Sci 2018;22:1285–98. https://doi.org/10.5194/hess-22-1285-2018.
[10] Adeh EH, Selker JS, Higgins CW. Remarkable agrivoltaic influence on soil moisture, micrometeorology and water-use efficiency. PloS One 2018;13. https://doi.org/10.1371/journal.pone.0203256.
[11] Valle B, Simonneau T, Sourd F, Pechier P, Hamard P, Frisson T, et al. Increasing the total productivity of a land by combining mobile photovoltaic panels and food crops. Appl Energy 2017;206:1495–507. https://doi.org/10.1016/j.apenergy.2017.09.113.
[12] Weselek A, Ehmann A, Zikeli S, Lewandowski I, Schindele S, Högy P. Agrophotovoltaic systems: applications, challenges, and opportunities. A review. Agron Sustain Dev 2019;39. https://doi.org/10.1007/s13593-019-0581-3.
[13] Dinesh H, Pearce JM. The potential of agrivoltaic systems. Renew Sustain Energy Rev 2016;54:299–308. https://doi.org/10.1016/j.rser.2015.10.024.
[14] Barron-Gafford GA, Pavao-Zuckerman MA, Minor RL, Sutter LF, Barnett-Moreno I, Blackett DT, et al. Agrivoltaics provide mutual benefits across the food–energy–water nexus in drylands. Nat Sustain 2019;2:848–55. https://doi.org/10.1038/s41893-019-0364-5.
[15] Williams HJ, Hashad K, Wang H, Max Zhang K. The potential for agrivoltaics to enhance solar farm cooling. Appl Energy 2023;332:120478. https://doi.org/10.1016/j.apenergy.2022.120478.
[16] Amaducci S, Yin X, Colauzzi M. Agrivoltaic systems to optimise land use for electric energy production. Appl Energy 2018;220:545–61. https://doi.org/10.1016/j.apenergy.2018.03.081.
[17] Scopus. https://www.scopus.com/; 2023 (accessed February 8, 2023).
[18] IEA PVPS. Task 1. Trends in Photovoltaic Applications — 2022. 2022.
[19] Enkhardt S. Global solar capacity additions hit 268 GW in 2022, says BNEF. PV Mag. https://www.pv-magazine.com/2022/12/23/global-solar-capacity-additions-hit-268-gw-in-2022-says-bnef/#:~:text=BloombergNEF; 2022. Analyst Jenny Chase says,hit 315 GW in 2023. (accessed February 7, 2023).
[20] Wimalasekera R. Effect of light intensity on photosynthesis. In: Ahmad P, Ahanger MA, Alyemeni MN, Alam P, editors. Photosynth. Product. Environ. Stress. Wiley; 2019. p. 65–73. https://doi.org/10.1002/9781119501800.ch4.
[21] Gorjian S, Bousi E, Özdemir ÖE, Trommsdorff M, Kumar NM, Anand A, et al. Progress and challenges of crop production and electricity generation in agrivoltaic systems using semi-transparent photovoltaic technology. Renew Sustain Energy Rev 2022;158:112126. https://doi.org/10.1016/j.rser.2022.112126.
[22] APC Group. Solar sharing for fun!. https://solar-sharing.org/sswp/wp-content/uploads/2018/08/1feb7cf46b50eece5b23cc808768e8c0.pdf; 2015.
[23] Trommsdorff M, Dhal IS, Özdemir ÖE, Ketzer D, Weinberger N, Rösch C. Agrivoltaics: solar power generation and food production. In: Sol. Energy Adv. Agric. Food Prod. Syst. Elsevier; 2022. p. 159–210. https://doi.org/10.1016/B978-0-323-89866-9.00012-2.
[24] Partnership for Research and Innovation in the Mediterranean Area (PRIMA). Drought, the silent enemy of the Mediterranean. https://prima-med.org/drought-the-silent-enemy-of-the-mediterranean/; 2023 (accessed March 22, 2023).
[25] Fernández EF, Villar-Fernández A, Montes-Romero J, Ruiz-Torres L, Rodrigo PM, Manzaneda AJ, et al. Global energy assessment of the potential of photovoltaics for greenhouse farming. Appl Energy 2022;309. https://doi.org/10.1016/j.apenergy.2021.118474.
[26] Edouard S, Combes D, Van Iseghem M, Ng Wing Tin M, Escobar-Gutiérrez AJ. Increasing land productivity with agriphotovoltaics: application to an alfalfa field. Appl Energy 2023;329. https://doi.org/10.1016/j.apenergy.2022.120207.
[27] Chae SH, Kim HJ, Moon HW, Kim YH, Ku KM. Agrivoltaic systems enhance farmers' profits through broccoli visual quality and electricity production without dramatic changes in yield, antioxidant capacity, and Glucosinolates. Agronomy 2022;12. https://doi.org/10.3390/agronomy12061415.
[28] Sekiyama T, Nagashima A. Solar sharing for both food and clean energy production: performance of agrivoltaic systems for corn, a typical shade-intolerant crop. Environ - MDPI 2019;6. https://doi.org/10.3390/environments6060065.
[29] Dupraz C, Marrou H, Talbot G, Dufour L, Nogier A, Ferard Y. Combining solar photovoltaic panels and food crops for optimising land use: towards new agrivoltaic schemes. Renew Energy 2011;36:2725–32. https://doi.org/10.1016/j.renene.2011.03.005.
[30] Marrou H, Guilioni L, Dufour L, Dupraz C, Wery J. Microclimate under agrivoltaic systems: is crop growth rate affected in the partial shade of solar panels? Agric For Meteorol 2013;177:117–32. https://doi.org/10.1016/j.agrformet.2013.04.012.
[31] Elamri Y, Cheviron B, Lopez JM, Dejean C, Belaud G. Water budget and crop modelling for agrivoltaic systems: application to irrigated lettuces. Agric Water Manag 2018;208:440–53. https://doi.org/10.1016/j.agwat.2018.07.001.
[32] Rollet C. A good year for solar: agrivoltaics in vineyards. PV Mag 2020.
[33] Malu PR, Sharma US, Pearce JM. Agrivoltaic potential on grape farms in India. Sustain Energy Technol Assessm 2017;23:104–10. https://doi.org/10.1016/j.seta.2017.08.004.
[34] Padilla J, Toledo C, Abad J. Enovoltaics: symbiotic integration of photovoltaics in vineyards. Front Energy Res 2022;10:1–11. https://doi.org/10.3389/fenrg.2022.1007383.
[35] Juillion P, Lopez G, Fumey D, Lesniak V, Génard M, Vercambre G. Shading apple trees with an agrivoltaic system: impact on water relations, leaf morphophysiological characteristics and yield determinants. Sci Hortic (Amsterdam) 2022;306. https://doi.org/10.1016/j.scienta.2022.111434.
[36] BayWa r.e. First Agri-PV Research Facility for Apples in Germany. Fraunhofer ISE. https://www.baywa-re.com/en/news/details/first-agri-pv-research-facility-for-apples-in-germany; 2021.
[37] Sousa AAR, Barandica JM, Aguilera PA, Rescia AJ. Examining potential environmental consequences of climate change and other driving forces on the sustainability of spanish olive groves under a socio-ecological approach. Agric 2020;10:1–22. https://doi.org/10.3390/agriculture10110509.
[38] Osorio-Aravena JC, Rodríguez-Segura FJ, Frolova M, Terrados-Cepeda J, Muñoz-Cerón E. How much solar PV, wind and biomass energy could be implemented in short-term? A multi-criteria GIS-based approach applied to the province of Jaén, Spain. J Clean Prod 2022;366. https://doi.org/10.1016/j.jclepro.2022.132920.
[39] Rodríguez-Segura FJ, Osorio-Aravena JC, Frolova M, Terrados-Cepeda J, Muñoz-Cerón E. Social acceptance of renewable energy development in southern Spain: exploring tendencies, locations, criteria and situations. Energy Policy 2023;173. https://doi.org/10.1016/j.enpol.2022.113356.
[40] Ciocia A, Enescu D, Amato A, Malgaroli G, Polacco R, Amico F, et al. Agrivoltaic system: a case study of pv production and olive cultivation in Southern Italy. In: 2022 57th Int Univ Power Eng Conf Big Data Smart Grids, UPEC 2022 - Proc; 2022. https://doi.org/10.1109/UPEC55022.2022.9917595.
[41] Bellini E. Integrating big solar into olive groves. PV Mag 2021.
[42] BayWa r.e. https://www.baywa-re.es/en/solar/projects/agri-pv#solutions; 2023 (accessed March 2, 2023).
[43] Food and Agriculture Organization of the United Nations (FAO). Production Quantities of Olives by Country. https://www.fao.org/faostat/en/#data; 2023 (accessed March 2, 2023).
[44] Fraga H, Moriondo M, Leolini L, Santos JA. Mediterranean olive orchards under climate change: a review of future impacts and adaptation strategies. Agronomy 2021;11:1–15. https://doi.org/10.3390/agronomy11010056.
[45] Palliotti A, Bongi G. Freezing injury in the olive leaf and effects of mefluidide treatment. J Hortic Sci 1996;71:57–63. https://doi.org/10.1080/14620316.1996.11515382.
[46] Gómez JA, Giráldez JV, Fereres E. Rainfall interception by olive trees in relation to leaf area. Agric Water Manag 2001;49:65–76. https://doi.org/10.1016/S0378-3774(00)00116-5.
[47] Moriondo M, Ferrise R, Trombi G, Brilli L, Dibari C, Bindi M. Modelling olive trees and grapevines in a changing climate. Environ Model Software 2015;72:387–401. https://doi.org/10.1016/j.envsoft.2014.12.016.
[48] Caudullo G, Welk E, San-Miguel-Ayanz J. Chorological maps for the main European woody species. Data Br 2017;12:662–6. https://doi.org/10.1016/j.dib.2017.05.007.
[49] European Commision. Photovoltaic geographical Information system (PVGIS). https://re.jrc.ec.europa.eu/pvg_tools/en/tools.html#MR; 2016.
[50] Ministerio de Agricultura Pesca y Alimentación. Aceite de oliva y aceituna de mesa. https://www.mapa.gob.es/es/agricultura/temas/producciones-agricolas/aceite-oliva-y-aceituna-mesa/balances.aspx; 2023 (accessed March 3, 2023).
[51] Castillo-Guerrero M. La cultura del olivo. Espac y Tiempo 2012;26:75–101.
[52] Productores aceite de oliva. https://aceites.top/productores-aceite-oliva/; 2023 (accessed March 3, 2023).
[53] Moroccan Olive Oil. Olive oil varieties. https://moroccanoliveoil.com/olive-oil/; 2023 (accessed March 3, 2023).
[54] Oliofficina. The Turkish olive oil sector. https://www.oliofficina.it/en/knowledge/economy/the-turkish-olive-oil-sector.htm; 2017 (accessed March 3, 2023).

[55] Boussahel S, Di Stefano V, Muscarà C, Cristani M, Melilli MG. Phenolic compounds characterization and antioxidant properties of monocultivar olive oils from Northeast Algeria. Agriculture 2020;10:494. https://doi.org/10.3390/agriculture10110494.
[56] Benincasa C, Russo A, Romano E. Chemical and sensory analysis of some Egyptian virgin olive oils. J Nutr Food Sci 2011;01. https://doi.org/10.4172/2155-9600.1000118.
[57] Radinovsky L. Everything you need to know about olive oil from Greece. https://www.oliveoil.com/everything-you-need-to-know-about-olive-oil-from-greece/; 2021.
[58] International Olive Council (IOC). Country profiles. https://www.internationaloliveoil.org/what-we-do/economic-affairs-promotion-unit/#country; 2023 (accessed March 3, 2023).
[59] Gómez-Escalonilla M, Vidal J. Variedades del olivar. Madrid. 2006.
[60] Khlif M, Ayadi M, Grati-Kammoun N, Arous MN, Rekik H, Hamdi MT, et al. Identifying chemlali olive variety in its traditional area. Acta Hortic 2002:117–20. https://doi.org/10.17660/ActaHortic.2002.586.16.
[61] Alentejo y el olivar superintensivo de Alqueva producen ya el 75% del aceite de oliva de Portugal. Rev Almaceite 2021.
[62] Martínez E. El cultivo intensivo de olivo en seto conquista España. La Razón 2022.
[63] Contreras MA. Más de la mitad del olivar de la provincia de Jaén «se puede modernizar y hacer más rentable». Ideal Jaén 2023.
[64] Super high density olive crops. https://www.agromillora.com/shd-olive-crops/; 2023 (accessed May 31, 2023).
[65] Swaid S, Appelbaum J, Aronescu A. Shading and masking of PV collectors on horizontal and sloped Planes facing south and north—a comparative study. Energies 2021;14:3850. https://doi.org/10.3390/en14133850.
[66] Chiteka K, Arora R, Sridhara SN, Enweremadu CC. Influence of irradiance incidence angle and installation configuration on the deposition of dust and dust-shading of a photovoltaic array. Energy 2021;216:1–10. https://doi.org/10.1016/j.energy.2020.119289.
[67] Wu B-S, Rufyikiri A-S, Orsat V, Lefsrud MG. Re-interpreting the photosynthetically action radiation (PAR) curve in plants. Plant Sci 2019;289:110272. https://doi.org/10.1016/j.plantsci.2019.110272.
[68] Micheli L, Fernandez EF, Smestad GP, Alrashidi H, Sarmah N, Sellami N, et al. A unified global investigation on the spectral effects of soiling losses of PV glass substrates: preliminary results. 2018. p. 2858–63. https://doi.org/10.1109/pvsc.2017.8366317.
[69] Holmgren F, Hansen W, Mikofski A. Pvlib Python: a Python package for modeling solar energy systems. J Open Source Softw 2018;3:884. https://doi.org/10.21105/joss.00884.
[70] Loutzenhiser PG, Manz H, Felsmann C, Strachan PA, Frank T, Maxwell GM. Empirical validation of models to compute solar irradiance on inclined surfaces for building energy simulation. Sol Energy 2007;81:254–67. https://doi.org/10.1016/j.solener.2006.03.009.
[71] Gomes L, Nobre T, Sousa A, Rei F, Guiomar N. Hyperspectral reflectance as a basis to discriminate olive varieties—a tool for sustainable crop management. Sustainability 2020;12:3059. https://doi.org/10.3390/su12073059.
[72] Bird R, Riordan C. Simple solar spectral model for direct and diffuse irradiance on horizontal and tilted planes at the earth's surface for cloudless atmospheres. Golden, CO. 1984. https://doi.org/10.2172/5986936.
[73] International Energy Agency (IEA). Greenhouse gas emissions from energy. https://www.iea.org/data-and-statistics/data-tools/greenhouse-gas-emissions-from-energy-data-explorer; 2022 (accessed March 8, 2023).
[74] Ram M, Osorio-Aravena JC, Aghahosseini A, Bogdanov D, Breyer C. Job creation during a climate compliant global energy transition across the power, heat, transport, and desalination sectors by 2050. Energy 2022;238:121690. https://doi.org/10.1016/j.energy.2021.121690.
[75] Plantaciones de olivos superintensivos. https://balam.es/services/plantaciones-llave-en-mano/plantacion-olivar/olivar-superintensivo/; 2023 (accessed May 31, 2023).
[76] Olivar intensivo y superintensivo: diferencias, cuidados y tratamiento. https://certisbelchim.es/olivar-intensivo-y-superintensivo-cuidados-y-tratamientos/#:~:text=Secalculaqueenel,laproducciónmundialdeolivares; 2023 (accessed June 13, 2023).
[77] SolarPower Europe. Global Market Outlook For Solar Power 2022–2026. Brussels, Belgium. 2022.
[78] Red Eléctrica de España. Potencia instalada - Sistema eléctrico: Nacional. https://www.ree.es/es/datos/generacion/potencia-instalada; 2023 (accessed February 14, 2023).
[79] Red Eléctrica de España. Generación renovable por tecnología. https://www.ree.es/es/datos/generacion/estructura-renovables; 2023 (accessed May 15, 2023).
[80] US Energy Information Administration. Electricity data. https://www.eia.gov/international/data/world/electricity/electricity-consumption; 2023.
[81] European Commission. REPowerEU: A plan to rapidly reduce dependence on Russian fossil fuels and fast forward the green transition. https://ec.europa.eu/commission/presscorner/detail/en/ip_22_3131; 2023 (accessed March 14, 2023).
[82] Ministerio para la Transición Ecológica y el Reto Demográfico. Plan Nacional Integrado de Energía y Clima 2021-2030. Minist Para La Transic Ecológica y El Reto Demográfico, Gob España. 2020. p. 25.
[83] European Commission. 2030 Climate Target Plan. https://climate.ec.europa.eu/eu-action/european-green-deal/2030-climate-target-plan_en; 2022 (accessed March 15, 2023).
[84] Crippa M, Guizzardi D, Banja M, Solazzo E, Muntean M, Schaaf E, et al. CO2 emissions of all world countries. 2022. https://doi.org/10.2760/07904.